Extraction of the Coulomb Sum Rule and Longitudinal Quasielastic Supression from an Analysis of Available e-^{12}C and e-^{16}O Cross Section Data.

A. Bodek[1] and M. E. Christy[2]

[1]*Department of Physics and Astronomy, University of Rochester, Rochester, NY 14627, USA*
[2]*Thomas Jeferson National Accelerator Facility, Newport News, VA 23606, USA*

(Dated: June 27, 2022)

We report on a phenomenological analysis of all available electron scattering data on $^{12}_{6}$C (about 8000 differential cross section measurements) and $^{16}_{8}$O (about 250 measurements) within the framework of the superscaling model (including Pauli blocking). All data are included down to the lowest momentum transfer $\vec{\mathbf{q}}$ including photo-production. We find that, in addition to the expected enhancement of the transverse quasielastic (QE) response function (R_T^{QE}), there is "Extra Suppression" of the QE longitudinal response function (R_L^{QE}) beyond that expected from Pauli blocking, and we extract a parameterization of the $|\vec{\mathbf{q}}|$ dependence of this "Extra Suppression". We additionally find that the nuclear excited states can contribute significantly (up to 30%) to the Coulomb Sum Rule $SL(\mathbf{q})$. All excited states have been fully included in the analysis to provide the most accurate determination of $SL(\mathbf{q})$ to date, which is compared to theoretical predictions.

We report on a fit to all electron scattering data on $^{12}_{6}$C (about 8000 differential cross section measurements) and $^{16}_{8}$O (about 250 measurements) within the framework of the superscaling model (including Pauli blocking). The fit includes empirical parameters to model the enhancement of the transverse quasielastic (QE) response function R_T^{QE}, and the suppression of the longitudinal response function R_L^{QE} as a function of momentum transfer $\vec{\mathbf{q}}$. The fit can be used to validate modeling of QE cross sections in current Monte Carlo event generators for electron and neutrino scattering. Careful consideration of nuclear excitations is critical for an accurate extraction of the Coulomb Sum Rule[1] (CSR) at low $\vec{\mathbf{q}}$ as these states can contribute up to 30%. After accounting for the nuclear excitations and including all available cross section data we have obtained the most accurate determination of CSR as function of $\vec{\mathbf{q}}$ for $^{12}_{6}$C and $^{16}_{8}$O and compared to theoretical models.

The suppression of the longitudinal QE cross section in electron scattering is also of interest to neutrino scattering experiments because recent neutrino experiments[2–5] on nuclear targets report suppression of the neutrino QE cross sections with respect to the predictions of Monte Carlo generators (which include Pauli blocking) at low values of $\mathbf{q}$. Additional suppression of the longitudinal QE response function at low $\mathbf{q}$ is expected in models[6] which also incorporate the effects of long range nucleon-nucleon correlations using the random phase approximation (RPA) and the electron scattering data can be used to investigate the this suppression (from all sources).

The electron scattering differential cross section can be written in terms of longitudinal, $R_L(\mathbf{q},\nu)$, and transverse, $R_T(\mathbf{q},\nu)$, response functions [7] as:

$$\frac{d\sigma}{d\nu d\Omega} \;=\; \sigma_M[AR_L(\mathbf{q},\nu) + BR_T(\mathbf{q},\nu)], \qquad (1)$$

where σ_M is the Mott cross section,

$$\sigma_M \;=\; \frac{\alpha^2\cos^2)(\theta/2)}{4E_0^2\sin^4(\theta/2)}. \qquad (2)$$

Here, E_0 is the incident electron energy, E' is energy of the final state electron, $\nu = E_0 - E'$ is the energy transfer to the target, $\mathbf{q}$ is the absolute value of the 3-momentum transfer, Q^2 is the square of the 4-momentum transfer (defined to be positive), $\mathbf{q^2}{=}Q^2+\nu^2$, $A = (Q^2/\mathbf{q^2})^{\mathbf{2}}$ and $B = \tan^2(\theta/2) + Q^2/2\mathbf{q^2}$.

The inelastic Coulomb Sum is the integral of $R_L(\mathbf{q},\nu)d\nu$, excluding the elastic peak and pion production processes. It has contributions from quasielastic scattering and from electro-excitations of nuclear states, such that

$$\begin{aligned}\mathrm{CSR}(\mathbf{q}) &= \int R_L(\mathbf{q},\nu)d\nu \qquad (3)\\ &= \int R_L^{QE}(\mathbf{q},\nu)d\nu + G_E'^2(q)\times Z^2\sum_{all}^{L}F_i^2(\mathbf{q})\\ &= G_E'^2(q)\times\big[Z\int V_L^{QE}(\mathbf{q},\nu)d\nu + Z^2\sum_{all}^{L}F_i^2(\mathbf{q})\big].\end{aligned}$$

$R_L^{QE}(\mathbf{q},\nu)$ is the longitudinal QE response and we define $V^{QE}(\mathbf{q},\nu)$ as the reduced longitudinal QE response, which integrates to unity in the absence of any suppression (e.g. Pauli blocking). The charge form factors for the electro-excitation of nuclear states ($F_{iC}^2(\mathbf{q})$) are the product of the spatial distribution form factor $F_i^2(\mathbf{q})$ times the the electric form factor of the proton $G_{E_p}'(\mathbf{q})$

In order to account for the small contribution of the neutron and for relativistic corrections $G_E'^2(q)$ is given by[7]:

$$G_E'^2(Q^2) = [G_{Ep}^2(Q^2) + \frac{N}{Z}G_{En}^2(Q^2)]\frac{1+\tau}{1+2\tau}, \qquad (4)$$

where, G_{Ep} and G_{En} are the electric form factors of the proton and neutron, respectively and $\tau = Q^2/4M_p^2$. We use the BBBA07 parameterizations [8] of the free nucleon form factors. At low Q^2 the quantity in brackets in equation 4 is well represented by a simple dipole $(1/(1+Q^2/0.71)^4)$.

By dividing Equation 3 by $ZG_E'^2\mathbf{q})$ we obtain the normalized inelastic Coulomb Sum Rule:

$$SL(\mathbf{q}) = \int V_L^{QE}(\mathbf{q},\nu)d\nu + Z\sum_{all}^{L} F_i^2(\mathbf{q}). \qquad (5)$$

At high $\mathbf{q}$ it is expected that $S_L \to 1$ because both the electro-excitation form factors and the Pauli suppression are small, while at small $\mathbf{q}$ it is expected that $S_L \to 0$ because of the Pauli suppression of V_L^{QE} and the fact that form factors for all nuclear excitations must be zero at $\mathbf{q}$=0.

We begin by using empirical fits to parameterize the measurements of the longitudinal and transverse form factors for the electro-excitation of all nuclear states in $^{12}_{6}$C with excitation energies less than 16.0 MeV (which is the removal energy of a proton from $^{12}_{6}$C). For these states the measurements are relatively straight forward since the QE cross section is zero. For excitation energies above 16 MeV the measurements require corrections for the QE contribution. We perform a reanalysis of all the published cross sections with excitation energies less than 55 MeV and use our own QE model (described below) and re-extract all the excitation form factors. For excitation energies above 20 MeV (region of the Giant Dipole resonance (GDR)) we group multiple excitations in wide bins of excitation energies and extract form factors in wider bins. As an example, Fig, 1 shows a comparison of our fit to some of longitudinal response functions measured by Yamaguchi 1996[9] for excitation energies above 16 MeV. The same analysis is done for $^{16}_{8}$O. The contributions of nuclear excitation to the Coulomb sum rule in $^{12}_{6}$C (factor $Z\sum_{all}^{L} F_i^2(\mathbf{q})$ in equation 5) is calculated using the our parametrizations for all the form factors. The top panel of Fig. 2 shows the contributions states (with excitation energies below 10 MeV, 20.5 MeV, 30 MeV and 55 MeV) to the Coulomb Rule for $^{12}_{6}$C. The same data for $^{16}_{8}$O is shown on the bottom panel. The contribution of all excited states is largest (about 0.29) at at $\mathbf{q}$=0.22 GeV.

The bottom panel of Fig. 2 shows the contribution of nuclear excitation to $SL(\mathbf{q})$ in $^{16}_{8}$O. Although the contributions of difference regions in excitation energy to the sum rule is different for $^{12}_{6}$C and $^{16}_{8}$O, the total contribution for $^{16}_{8}$O is consistent with being the dame as for $^{12}_{6}$C.

The analysis of the $^{12}_{6}$C data is based on a 2021 update of the 2012 fit by Bosted and Mamyan [10]. We include all available data down to the lowest $\mathbf{q}$. The overall fit models the QE contribution using the superscaling approach[11–14] with Pauli blocking using the Rosenfelder[14–16] method. The superscaling function

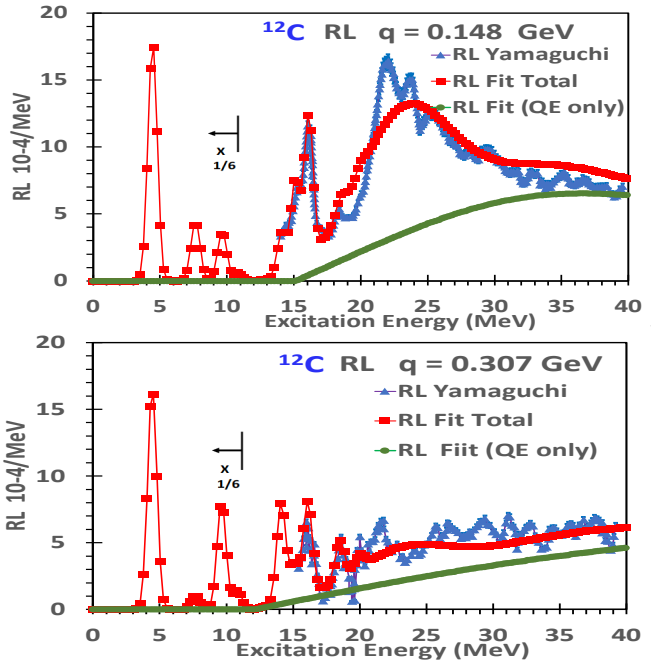

FIG. 1: Comparison of our fit to $R_L(\mathbf{q},\nu)$ for $^{12}_{6}$C to some of the experimental data of Yamaguchi 1996 [9]. For excitation energies less than 12 MeV the cross the values are multiplied by '1/6.

that we extract from the fit is similar to the superscaling functions of Amaro 2005[12] and Amaro 2020[13] and yields similar values of the Pauli suppression.

In modeling the QE we use the same scaling function for both the longitudinal and transverse contributions and fit for empirical parametrizations of corrections to the transverse and longitudinal response functions. For R_T^{QE} we extract an *additive* "Transverse Enhancement/MEC" TE$(\mathbf{q},\nu)$ contribution (which includes both single nucleon and two nucleon final states) as discussed in ref.[17]. For R_L^{QE} we extract a multiplicative $\mathbf{q}$ dependent "Extra Suppression" factor $F_{extra}(\mathbf{q})$. The TE$(\mathbf{q},\nu)$ additive contribution increases R_T^{QE} with the largest fractional contribution around Q^2=0.3 GeV^2. In contrast, the "Extra Suppression" multiplicative factor decreases R_L^{QE} at low values $\mathbf{q}$. Since the cross section measurements span a large range of θ and Q^2, parametrizations of both the transverse TE$(\mathbf{q},\nu)$ and the longitudinal $F_{extra}(\mathbf{q})$ can be extracted from the fit. The 2021 updated analysis includes all data for a large range of nuclei. However, in this analysis we only include data on $^{12}_{6}$C. Briefly, the updated fit includes the following:

1. All available electron scattering data on hydrogen, deuterium and $^{12}_{6}$C QE in addition to what is available in the QE archive[18]

2. Coulomb corrections[19] using the Effective Momentum approximation (EMA) are included in modeling scattering from nuclear targets.

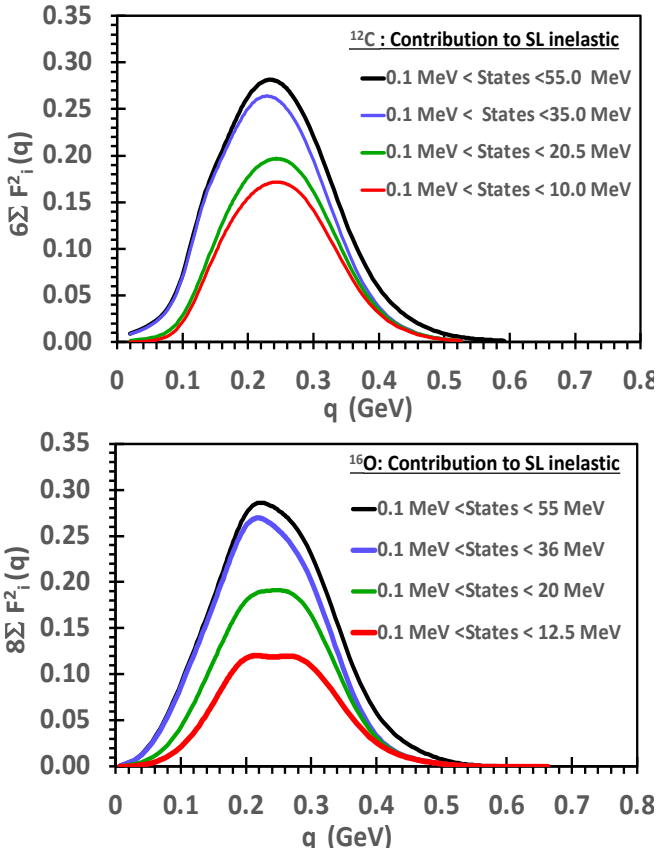

FIG. 2: The contributions of longitudinal nuclear excitations (between 2 and 55 MeV) to the Coulomb sum rule ($Z\sum_{all}^{L} F_i^2(\mathbf{q})$) in equation 5 for $^{12}_{6}$C (top panel) and $^{16}_{8}$O (bottom panel).

3. Updated $^{12}_{6}$C nuclear elastic form factor.

4. $^{12}_{6}$C nuclear excitations form factors.

5. Superscaling $FN(\psi')$ parameters are re-extracted including the Fermi broadening parameter K_F.

6. The parameterizations of the free nucleon form factors[20] are re-derived from all available deuterium and hydrogen data.

7. Rosenfelder Pauli suppression[14–16] which reduces and changes the QE distribution at low $\mathbf{q}$ and ν.

8. A $\mathbf{q}$ dependent $E^{QE}_{\rm shift}(\mathbf{q})$ parameter for the QE process to account for the optical potential[21] of final state nucleons. $E^{QE}_{\rm shift}(\mathbf{q})$ is constrained to be greater than 16 MeV, which is the separation energy of a proton from $^{12}_{6}$C. For $\mathbf{q}$ <1 GeV we use $E_{shift}(GeV) = 0.020 - 0.004\sqrt{1-\mathbf{q}}$, and for $\mathbf{q}$ >1 we use E_{shift} (GeV) =0.020.

9. Updated fits[20] to inelastic electron scattering data (in the nucleon resonance region and inelastic pion production continuum) for hydrogen and deuterium.

10. Photo-production data in the nucleon resonance region and inelastic pion production continuum[22].

11. Updated Gaussian Fermi smeared nucleon resonance and inelastic pion production[22]. The Fermi broadening parameter for inelastic pion production can be different from the QE ψ' Fermi broadening parameter.

12. Parametrizations of the medium modifications of both the transverse and longitudinal structure functions responsible for the EMC effect (nuclear dependence of Deep Inelastic Scattering). This is applied to the free nucleon prior to application of the Fermi smearing.

13. Updated parameters of the contribution of the "Transverse Enhancement/MEC".

14. Parameters to account for low $\mathbf{q}$ suppression of the longitudinal response function.

15. QE data at *all values* of Q^2 down to Q^2=0.01 GeV^2 ($\mathbf{q}$=0.1 GeV) (which were not included in the Bosted-Mamyan fit).

As an example, Fig. 3 Shows a comparison of electron scattering differential cross sections[18, 23, 24] at $\mathbf{q}$ values close to 0.30, 0.38 and 0.57 GeV and at different scattering angle to our fit. The total (differential) cross section is shown as the solid purple line. The total minus the contribution of the nuclear excitations is shown as the solid blue line. The QE differential cross section (without TE) is the dashed blue line. The TE contribution is shown as the solid red line. Pion production processes (labeled inelastic) are shown as the dot-dashed black line. The fit is in good agreement with the data for both small and large angles

The left panel of Figure 4 shows a comparison of the extracted $^{12}_{6}$C $SL^{data}(\mathbf{q})$ (dotted black curve with yellow band) to three theoretical calculations for $^{12}_{6}$C. These include the Lovato 2016[25] "First Principle Green's Function Monte Carlo" calculation (solid purple line). An earlier Mihaila[26] 2000 Coupled-Clusters based calculation (AV18+UIX potential, dotted green line), and a recent Cloet 2016[6] RPA based calculation (RPA solid red line). Our results are consistent with, but somewhat lower than Lovato 2016 and are in poor agreement with the Mihaila 2000 and Cloet 2016 calculations

There is not enough experimental QE data for $^{16}_{8}$O to perform a complete analysis. The Fermi parameters for $^{12}_{6}$C and $^{16}_{8}$O are similar and the fit parameters for $^{12}_{6}$C should also describe all available data on $^{16}_{8}$O. We find that the fit parameters for $^{12}_{6}$C also describe all available data on $^{16}_{8}$O. A difference in $SL(\mathbf{q})$ between $^{12}_{6}$C and $^{16}_{8}$O could be the contribution of nuclear excitations. However as shown in Fig. 2 the contributions of nuclear excitations to the Coulomb sum rule for $^{12}_{6}$C and $^{16}_{8}$O are consistent with being equal.

The right panel of the bottom of Fig. 4 shows $SL^{data}(\mathbf{q})$ for $^{16}_{8}$O (dotted black curve with green band)

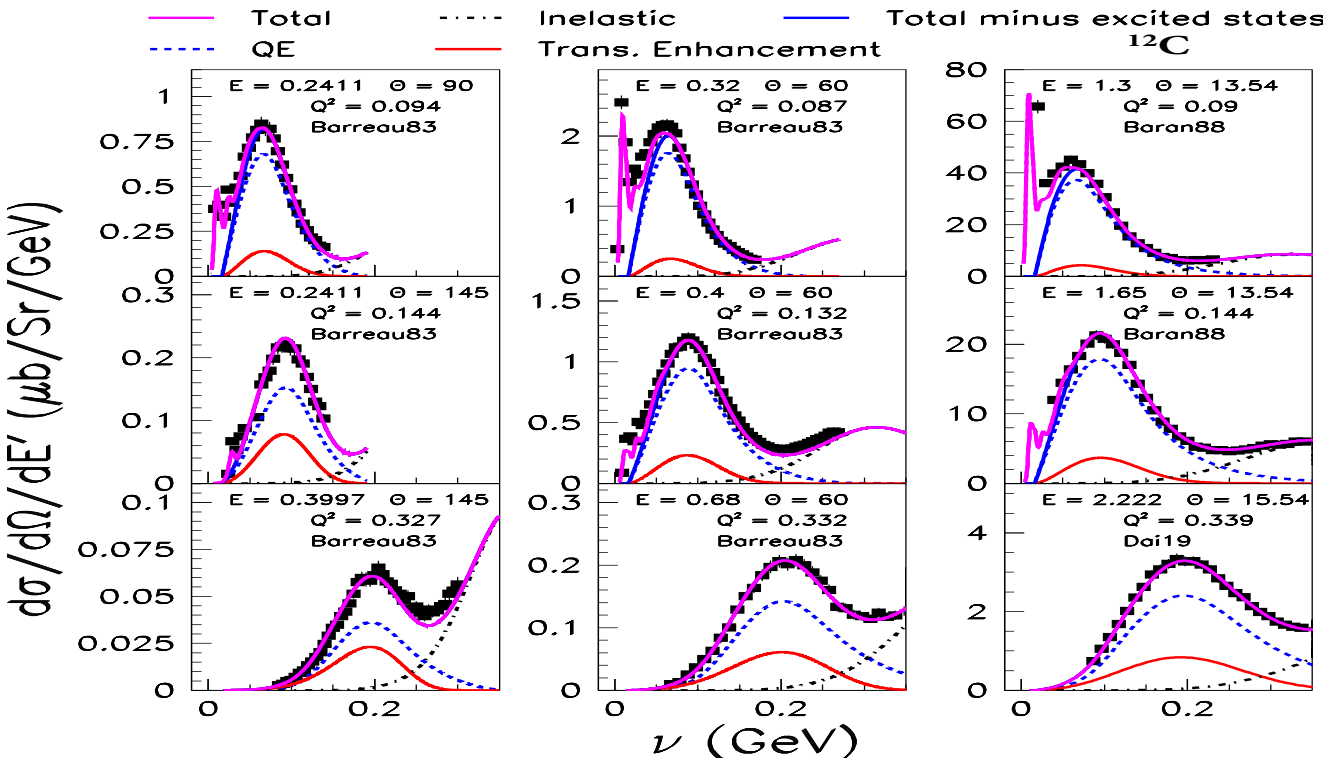

FIG. 3: Comparison of electron scattering differential cross sections[18, 23, 24] at **q** values close to 0.30, 0.38 and 0.57 GeV and at different scattering angle to our fit. The total (differential) cross section is shown as the solid purple line. The total minus the contribution of the nuclear excitations is shown as the solid blue line. The QE differential cross section (without TE) is the dashed blue line. The TE contribution is shown as the solid red line. Pion production processes (labeled inelastic) are shown as the dot-dashed black line. The fit is in good agreement with the data for both small and large angles.

compared to theoretical calculations for $^{16}_{8}$O. The calculations include the Sobczyk 2020 [27] "Coupled-Cluster with Singles-and Doubles (CCSD) NNLO$_{sat}$" (red dashed line), and an earlier Mihaila 2000[26] Coupled-Cluster calculation with (AV18+UIX potential, dotted green line). The data are consistent with but somewhat above the Sobczyk 2020 CCSD NNLO$_{sat}$ calculation for $^{16}_{8}$O and are in poor agreement with the Mihaila 2000 calculation.

In summary, we find that at low values of **q** there is "Extra Suppression" of the longitudinal QE response function in addition to the expected suppression from Pauli blocking. We obtain the best measurement of the Coulomb Sum Rule $SL(\mathbf{q})$ as function of $\vec{\mathbf{q}}$. $SL(\mathbf{q})$ for $^{12}_{6}$C is consistent with but somewhat lower than Lovato 2000 "First Principle Green's Function MC" calculations. $SL(\mathbf{q})$ for $^{16}_{8}$O is consistent with but somewhat higher than the Sobczyk 2020 "coupled-cluster with singles-and doubles (CCSD) NNLO$_{sat}$ " calculation.

The contribution of nuclear excitations to $SL(\mathbf{q})$ is significant (up to 29%). Theoretical studies of the excitation of nuclear states in neutrino scattering[28, 29] indicate that the excitations of nuclear states in neutrino scattering at low values of **q** are also significant. Therefore, nuclear excitations should be included in both electron and neutrino MC generators. We note that for excitation energies above proton removal threshold the decays of nuclear nuclear excitations can have a proton in the final state and therefore cannot be distinquished from QE events in neutrino experiments.

Currently, two long articles detailing the various components of the analysis are in preparation. This Research is supported by the U.S. Department of Energy, Office of Science, under University of Rochester grant number DE-SC0008475, and the Office of Science, Office of Nuclear Physics under contract DE-AC05-06OR23177.

[1] D. Drechsel and M M Giannini 1989 Rep. Prog. Phys. 52 1083 (eq. 7.9); T. de Forest Jr. and J.D. Walecka, Advances in Physics, 15:57, 1-109 (1966) (eq. 6.8).
[2] A. A. Aguilar-Arevalo et. al.,. (MiniBooNE) Phys. Rev. Lett. 100, 032301 (2008).
[3] M. F. Carneiro et. al.,. (MINERvA Collaboration), Phys. Rev. Lett. 124, 121801 (2020).
[4] P. Abratenko et. al.,. (MicroBooNE), Phys. Rev. Lett. 123, 131801 (2019).
[5] P. Abratenko et. al.,. (MicroBooNE) Phys. Rev. Lett.

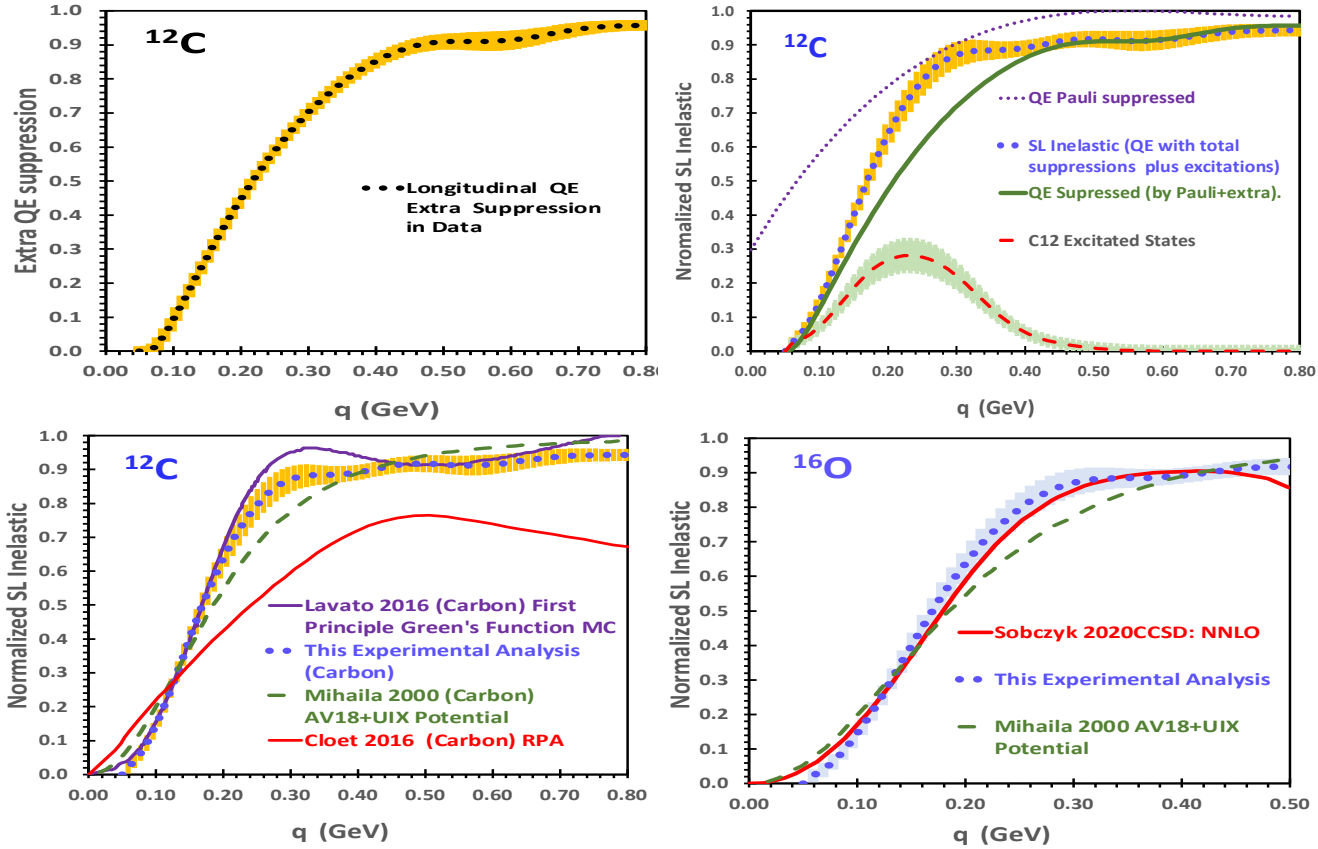

FIG. 4: Top left panel: Longitudinal "Extra Suppression" factor (beyond Pauli suppression in the Christy superscaling model) extracted from data) is shown in the black dotted line versus **q**. The yellow band corresponds to the statistical error from the fit, with a systematic error of 0.015 (added in quadrature) to account for the choice of parametrization function. Top right panel: The various contributions to the measured "Inelastic Coulomb Sum Rule" $SL(\mathbf{q})$ for $^{12}_{6}$C (shown as the dotted black line). The solid blue line is the Pauli suppressed QE. The solid green line is the contribution of $\int V_L^{QE}(\mathbf{q},\nu)d\nu$ from the data suppressed by both "Pauli Suppression" and the additional "Extra QE Suppression" extracted from the data (labeled QE total suppression). The red dashed line is the contribution of the nuclear excitations to the sum rule (the error band is 15% plus 0.01 added in quadrature). Bottom left panel: $\mathrm{SL}^{data}(\mathbf{q})$ for $^{12}_{6}$C (dotted black curve with yellow band) compared to theoretical calculations for $^{12}_{6}$C including "First Principle" Green's Function Monte Carlo [25] calculation (Lovato 2016, solid purple line), an earlier Coupled-Cluster [26] calculation (Mihaila 2000 AV18+UIX potential dotted green line), and an RPA based[6] calculation (Cloet 2016 RPA solid red line). Bottom right panel: $SL^{data}(\mathbf{q})$ for $^{12}_{6}$C (dotted black curve with green band) compared to theoretical calculations for $^{16}_{8}$O including Sobczyk 2020 [27] "coupled-cluster with singles-and doubles (CCSD) NNLO$_{sat}$ calculation (red dashed line), and an earlier Coupled-Cluster [26] calculation (Mihaila 2000 AV18+UIX potential dotted green line).

125, 201803 (2020)

[6] Ian C. Cloet, Wolfgang Bentz, Anthony W. Thomas, Phys. Rev. Lett. 116, 032701 (2016)

[7] J.A. Caballero, M. C. Martinez, J. L. Herraiz, J.M. Udias Physics Letters B 688. 250 (2010).

[8] A. Bodek, S. Avvakumov, R. Bradford, H. Budd, Eur. Phys. J C53, 349 (2008).

[9] Y. Yamaguchi et. al.,., Phys. Rev. D3, 1750 (1971).

[10] P.E. Bosted and V. Mamyan, arXiv:1203.2262 (2012); V. Mamyan, Ph.D. dissertation, Univ. of Virginia, 2010.

[11] C. Maieron, T.W. Donnelly, I. Sick, Phys.Rev. C65 (2002) 025502

[12] J.E. Amaro, M.B. Barbaro, J.A. Caballero, T.W. Donnelly, A. Molinari, and I. Sick, Phys. Rev. C 71, 015501 (2005)

[13] J.E. Amaro, M.B. Barbaro, J.A. Caballero, R. Gonzalez-Jimenez, G.D. Megias, I. Ruiz Simo, J. Phys. G: Nucl. Part. Phys. 47 124001 (2020

[14] G.D. Megias Vazquez (Tesis Doctoral). Universidad de Sevilla, Sevilla (2017)

[15] R. Rosenfelder, Ann. Phys. 128, 188 (1980).

[16] G. D. Megias et. al.,. Phys. Rev. D 89, 093002 (2014).

[17] A. Bodek, H. Budd, snd M. Christy, Eur.Phys.J.C 71 (2011) 1726

[18] O. Benhar, D. Day and I. Sick, Rev. Mod. Phys. 80, 189, 2008. Quasielastic Electron Nucleus Scattering Archive. http://faculty.virginia.edu/qes-archive/

[19] P. Gueye et. al.,. Phys. Rev. C60, 044308 (1999)

[20] P.E. Bosted, Phys. Rev. C 51, 409 (1995).

[21] Arie Bodek and Tejin Cai, Eur. Phys. J. C. (2019) 79; Arie Bodek and Tejin Cai, Eur. Phys. J. C 80, 655 (2020).

[22] P.E. Bosted and M.E. Christy, Phys. Rev. C 77, 065206 (2008); M.E. Christy and P.E. Bosted, Phys. Rev. C 81, 055213 (2010).

[23] P. Barreau et. al., Nucl. Phys. 402A (1983) 515.

[24] D. T. Baran et. al.,, Phys, Rev. Lett. 61 (1988) 400.

[25] A. Lovato et. al, Phys. Rev. Lett. 117, 082501 (2016)
[26] Bogdan Mihaila and Jochen H. Heisenberg, Phys, Rev. Lett. 84 (2000) 1403. 2009.01761 [nucl-th]
[27] J. E. Sobczyk, B. Acharya, S. Bacca, and G. Hagen Phys.Rev.C 102 (2020) 064312
[28] V. Pandey, N. Jachowicz, T. Van Cuyck, J. Ryckebusch, and M. Martini, Phys. Rev. C 92, 024606 (2015)
[29] M. Martini, N. Jachowicz, M. Ericson, V. Pandey, T. Van Cuyck, and N. Van Dessel, Phys. Rev. C 94, 015501 (2016); V. Pandey et al. Phys. Rev. C 94, 054609 (2016).